Intermetallics 125 (2020) 106922

Contents lists available at ScienceDirect

Intermetallics

journal homepage: http://www.elsevier.com/locate/intermet

Unified perspective on structural heterogeneity of a LaCe-based metallic glass from versatile dynamic stimuli

Z.R. Xu [a], D.S. Yang [a], J.C. Qiao [a,*], J.M. Pelletier [b], D. Crespo [c], E. Pineda [c], Yun-Jiang Wang [d,e,**]

[a] School of Mechanics, Civil Engineering and Architecture, Northwestern Polytechnical University, Xi'an, 710072, China
[b] Université de Lyon, MATEIS, UMR CNRS5510, Bat. B. Pascal, INSA-Lyon, F-69621, Villeurbanne Cedex, France
[c] Departament de Física, Barcelona Research Center in Multiscale Science and Technology & Institut de Tècniques Energètiques, Universitat Politècnica de Catalunya, 08019, Barcelona, Spain
[d] State Key Laboratory of Nonlinear Mechanics, Institute of Mechanics, Chinese Academy of Sciences, Beijing, 100190, China
[e] School of Engineering Science, University of Chinese Academy of Sciences, Beijing, 101408, China

ARTICLE INFO

Keywords:
Metallic glass
Structural heterogeneity
Dynamic mechanical relaxation
Stress relaxation
Creep

ABSTRACT

Dynamic mechanical relaxation, stress relaxation and creep were performed in a $La_{56.16}Ce_{14.04}Ni_{19.8}Al_{10}$ metallic glass with pronounced β relaxation features. The evolution of the microstructural heterogeneity with temperature is indirectly revealed via dynamic heterogeneity and analyzed in terms of several independent theoretical approaches. An apparent activation energy of β relaxation is obtained by assuming the Arrhenius relationship, which is calibrated by either the activation enthalpy of stress relaxation or the activation energy of creep. It is found that similar deformation mechanisms accommodate the dynamics of the LaCe-based metallic glass under different types of external stimuli applied in mechanical experiments.

1. Introduction

Compared with conventional metallic materials, metallic glasses (MGs) exhibit excellent mechanical, chemical and physical properties [1–4]. However, it is well known that the deformation theory of conventional crystalline solids, which is based on their intrinsic structural defects such as dislocations and grain boundaries [5], fails to describe the deformation mechanism of glassy solids [6]. Moreover, since the plastic deformation of MGs at room temperature is highly localized in shear bands, the lack of macroscopic plasticity has become a great obstacle to the application of these materials. In recent years, some studies have shown that the plastic deformability of MG can be effectively improved by introducing crystalline phases, which brings good news for the research in this field [7–10]. Nevertheless, the definition of "defects" in MGs and the correlation between their mechanical properties and microstructure are now undergoing and are still under hot discussion [6,11–13]. Structural heterogeneity in MGs has been verified with the help of experimental, computational, and theoretical investigations [14–17]. Specifically, structural heterogeneity of MGs is on the origin of the glass transition, diffusion behavior, mechanical properties, mechanical relaxation process and crystallization behavior [18,19].

Zhu et al. proposed that the origin of the β relaxation, namely, Johari–Goldstein secondary relaxation in MG is also the structural heterogeneity [20]. MGs with pronounced β relaxation modes usually tend to show conspicuous heterogeneous microstructure [21,22]. From the perspective of deformation, the shear transformation zones (STZs) model proposed by Argon [23] has become the mainstream framework to explain the plastic deformation behavior of MGs. Yu et al. reported that the activation energy E_β of the β relaxation in MGs is related to the potential energy barriers of the STZs: W_{STZ}, i.e., $E_\beta \approx W_{STZ}$ [21], which indicates that the β relaxation and the dynamics of STZs have the same origin at the microstructural scale [24]. Besides, it is well accepted that β relaxation, tensile plasticity and structural heterogeneity in MGs are strongly correlated, which makes the research on the features of structural heterogeneity a subject of great significance [16,19,21,24]. Then a question which naturally arises is how to unify the mechanism of relaxation and deformation in the general glasses.

In the current work, a typical La-based MG with an evident slow β relaxation process was chosen as a model alloy to explore the nature of relaxation and deformation of glasses [18,25]. Dynamic mechanical analysis (DMA) allows us to determine the apparent activation energy of

* Corresponding author.
** Corresponding author.
E-mail addresses: qjczy@nwpu.edu.cn (J.C. Qiao), yjwang@imech.ac.cn (Y.-J. Wang).

https://doi.org/10.1016/j.intermet.2020.106922
Received 1 June 2020; Received in revised form 17 July 2020; Accepted 25 July 2020
Available online 11 August 2020

the slow β relaxation according to the classical Arrhenius equation. Stress relaxation is able to probe the evolution of structural heterogeneity with temperature, as it is well described by the so-called stretched exponential Kohlrausch-Williams-Watts (KWW) equation [26]. This model accounts for the evolution of the effective relaxation time τ_c and, in particular, the stretching parameter β_{KWW} which is a signature of the degree of dynamic heterogeneity. Finally, creep experiments were performed and analyzed by means of the free volume model [27], allowing one to determine the activation volume. The apparent activation energy of creep Q_{app} was also calculated; interestingly, it is proved that Q_{app} is similar to the activation energy of slow β relaxation E_β. The characteristic relaxation times of the creep process were also determined by fitting to a distribution of discrete relaxation times. Combining the whole set of data one can speculate that β relaxation process, stress relaxation and creep have a similar physical origin, namely, the structural heterogeneity in MGs.

2. Experimental procedures

$La_{56.16}Ce_{14.04}Ni_{19.8}Al_{10}$ (at. %) bulk MG was prepared by copper mold suction casting in a high-purity argon atmosphere. The master alloy was remelted at least 6 times to ensure its chemical homogeneity. The glassy nature of the alloy was examined by X-ray diffraction (XRD, Philips PW3830) with Cu-Kα radiation. The thermal properties of $La_{56.16}Ce_{14.04}Ni_{19.8}Al_{10}$ MG were determined by differential scanning calorimeter (DSC, NEZTCH 404C) under a high-purity nitrogen atmosphere with a heating rate of 10 K/min. The dynamic mechanical behaviors of $La_{56.16}Ce_{14.04}Ni_{19.8}Al_{10}$ MG were studied by the DMA, TA Q800 in single-cantilever bending mode. DMA experiments (dimension of the samples: 30 mm × 2 mm × 1 mm) were carried out in a nitrogen-flushed atmosphere. The storage $E^{'}$ and loss $E^{''}$ moduli of the materials were obtained by the DMA measurements. Creep and stress relaxation experiments were performed on ribbons prepared by high-vacuum melt spinning from the master alloy. Both creep and stress relaxation tests were carried out using the same DMA analyzer in tensile mode. Creep tests were conducted at the temperatures of 315, 330, 350 and 370 K, respectively. Stress relaxation tests were performed over a large temperature range (from 308 to 413 K) with a constant strain of 0.4%. The characteristic relaxation times of the creep experiments were fitted to a set of 40 constant relaxation times, τ_i, in geometrical progression, so as $\tau_{i+1} = \gamma\tau_i$ with $\tau_0 = 1$ s and $\gamma = 10^{0.25} = 1.778$. The full range of fitted relaxation times covers a range of 10 orders of magnitude. The so-called "elastic net" procedure [28] was used for fitting in order to find maximum likelihood estimators.

The glassy nature of $La_{56.16}Ce_{14.04}Ni_{19.8}Al_{10}$ bulk MG and ribbon samples were verified by XRD (as shown in Fig. 1(a)). The thermal properties of the analyzed alloys were measured by DSC (as shown in Fig. 1(b)). The glass transition temperature T_g and the onset crystallization temperature T_x are also indicated in Fig. 1(b). These results are in good accordance with the previous literature [29].

3. Results and discussion

We begin the presentation of our results with investigating the mechanical relaxation behavior of $La_{56.16}Ce_{14.04}Ni_{19.8}Al_{10}$ bulk MG. Fig. 1 (c) shows the normalized storage modulus $E^{'}$ and loss modulus $E^{''}$ as a function of temperature (heating rate: 3 K/min, driving frequency: 1 Hz). It must be noted that an evident slow β relaxation process takes place at around 330 K. Moreover, at lower temperatures, around 250 K, a notable fast $\beta^{'}$ relaxation peak can be seen. It should be stressed that a pronounced faster $\beta^{'}$ relaxation in rare earth based amorphous alloys has been extensively detected [5]. Compared with slow β relaxation, fast $\beta^{'}$

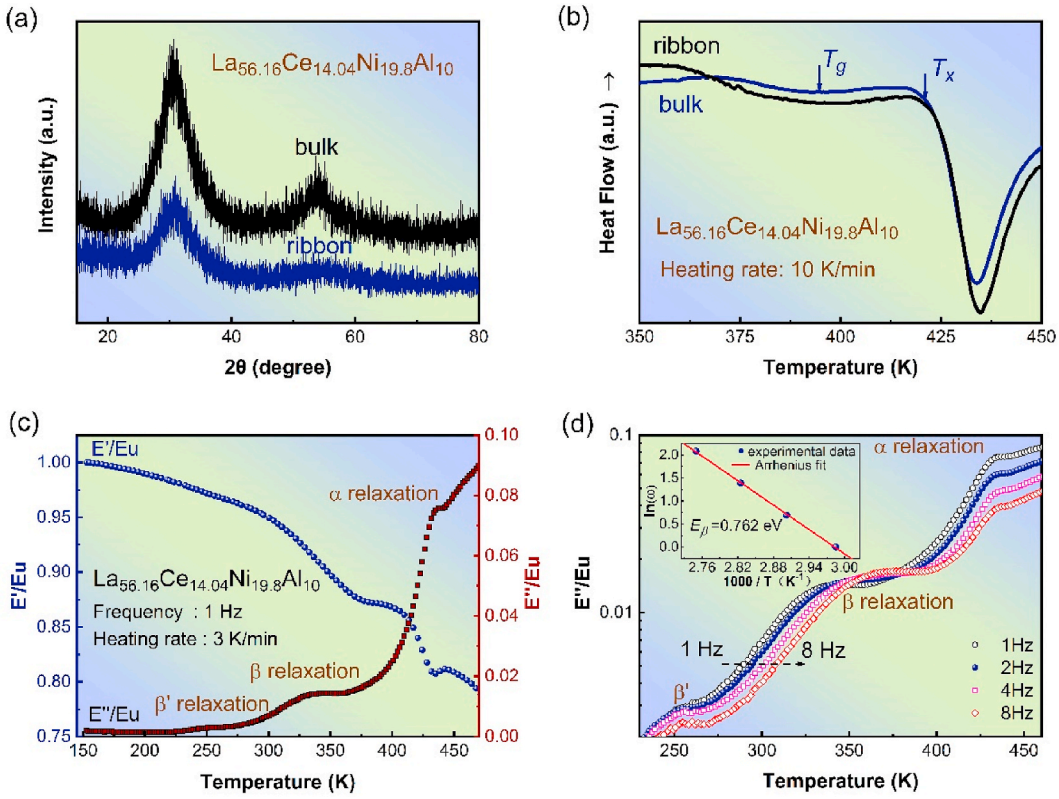

Fig. 1. (a) XRD patterns of $La_{56.16}Ce_{14.04}Ni_{19.8}Al_{10}$ MG (bulk and ribbon samples); (b) DSC curves of the same materials at a heating rate of 10 K/min; (c) Temperature dependence of the normalized storage and normalized loss moduli (bulk sample) at a heating rate of 3 K/min (driving frequency of 1 Hz); (d) Temperature dependence of the normalized loss modulus (bulk sample) at different frequencies (1, 2, 4 and 8 Hz, respectively). The inset displays the Arrhenius plot of the peak frequency of loss modulus along the slow β relaxation versus the reciprocal temperature.

relaxation only needs a smaller activation energy to drive. It is generally postulated that fast β' relaxation corresponds to the movement of a few atoms with high mobility, while the slow β relaxation involves a slightly larger number of atoms [5,30]. As the temperature continues to rise, a significant peak appears on the DMA spectrum, which is related to the primary (α) relaxation. The α relaxation is the main relaxation mode, and their activation denotes the onset of the dynamic glass transition. Different from the β relaxation which is associated with local, sometimes reversible, motion of small-scale atoms in the system, the α relaxation is due to irreversible, large-scale cooperative motion of atoms [5,31]. Related research also manifests that the intensity of the α relaxation is usually around ten times that of slow β relaxation [5].

Around 440 K, the tendencies of storage and loss moduli denote the onset of crystallization. It should be additionally pointed out that the forms of structural relaxation of the MG composites incorporating ductile dendrite phases are conspicuously different from that of conventional MGs. Owing to the complicated phase transition process during heating, the material tends to exhibit abnormal internal friction behavior within a specific temperature range [32]. Besides, the introduction of crystal phases decrease the mobility of atoms inside the material, resulting in a corresponding weakening of the intensity of α relaxation [33].

In order to further test the influence of frequency on the slow β relaxation process of $La_{56.16}Ce_{14.04}Ni_{19.8}Al_{10}$ bulk MG, isochronal measurements were carried out at different driving frequencies (1, 2, 4 and 8 Hz, respectively). Fig. 1(d) exhibits the temperature dependence of the normalized loss modulus at various driving frequencies. The peak of the slow β relaxation shifts to higher temperatures with increasing driving frequency. According to the Arrhenius equation $\omega = \omega_0 exp[-E_\beta/(k_BT)]$, where ω_0 is an exponential pre-factor of the order of the Debye frequency, E_β is the apparent activation energy of the slow β relaxation, k_B is the Boltzmann constant, and T is the temperature of the measurement. The activation energy of the slow β relaxation can be determined to be $E_\beta = 0.762$ eV. Taking into consideration the glass transition temperature T_g (as shown in Fig. 1(a)), we further see that $E_\beta/(k_BT_g) = 22.2$, which is in good agreement with the empirical scaling law between the activation energy of β relaxation and the glass transition temperature of a wide range of glasses, i.e., $E_\beta \approx 24k_BT_g$ [21].

Stress relaxation and creep are the usual mechanical stimuli adequate to probe the structural heterogeneity in MGs [34–37]. Fig. 2(a) shows the isothermal stress relaxation spectra of $La_{56.16}Ce_{14.04}Ni_{19.8}Al_{10}$ within a large temperature window (temperatures from 308 to 413 K, temperature interval is 5 K). It can be seen that the stress decreases first rapidly and then evolves more and more slowly with time. Moreover, as the test temperature gradually increases, it can be observed that the final equilibrium stress (at infinite time) tends to take a smaller value, which reflects the nature of activation process of the deformation units inside the MG. With the increasing temperature, more deformation units have been activated in the specimen, allowing more volume fraction of MG to undergo inelastic deformation [38]. It is well documented that the intrinsic nature of the deformation units in MGs can be described in the framework of the structural heterogeneity, modeled as free volume [27], flow units [39,40], liquid-like regions [41,42] or quasi-point defects [43,44], etc.

In addition, the stress relaxation process in MG can be described by a stretched exponential, or the Kohlrausch-William-Watts(KWW) equation [26]:

$$\varphi(t) = \frac{\sigma(t)}{\sigma_0} = exp\left[\left(-\frac{t}{\tau_c}\right)^{\beta_{KWW}}\right], \quad (1)$$

where τ_c is the characteristic relaxation time, and β_{KWW} is a stretching parameter ranging from 0 to 1. The stretching parameter β_{KWW} characterizes the distribution width of the relaxation times, which is a direct signature of dynamic heterogeneity and is related to the structural heterogeneity of MGs [38,45]. Fig. 2(b) exhibits the variation of the parameters fitted by the KWW equation τ_c and β_{KWW} with temperature. The characteristic relaxation time τ_c of the KWW model decreases rapidly with increasing temperature, which further corroborates our viewpoint that under the condition of higher test temperature, the deformation units are easier to be activated. On the other hand, the β_{KWW} exponent has a value around 0.77 within the temperature range of β relaxation, and after a decrease it increases swiftly when the temperature exceeds the glass transition temperature. As aforementioned, β_{KWW} is a parameter indirectly reflecting the structural heterogeneity of a metallic glass system. When the parameter is close to 1, the MG system is more homogeneous, and it decreases as the heterogeneity increases [45,46]. When the stress relaxation is carried out around the β relaxation region, only a small number of atom clusters are activated and undergo reversible or irreversible local atomic rearrangement. As the temperature continues to increase, and finally above T_g, the main α relaxation process starts to dominate the dynamics, corresponding to irreversible large-scale cooperative motions of atoms [25]. Consequently, it results in the emergence of a more homogeneous structure at high temperatures.

DMA and stress relaxation probe the glass in the same temperature range. Stress relaxation can be understood as DMA with an infinite period, which we will refer as quasi-null frequency. The time-temperature-superposition principle has been successfully applied in the analysis of the dynamic mechanical properties of glasses in temperature ranges where the glass topology does not change due to structural transformations [47]. Here we intend to extend this principle to the data obtained at quasi-null frequency. Fig. 2(c) shows the values of the bulk modulus determined by DMA at different frequencies with an individually adjusted temperature shift as a function of the main relaxation time τ_c fitted to the static relaxation curves in the temperature range between 308 and 423 K. The decrease on the bulk modulus at increasing temperatures shows a clear correlation with the logarithm of the main relaxation time τ_c of the KWW fitting, which reveals how the activation of flow units [35] with temperature is simultaneously responsible for the reduction of the bulk modulus and the relaxation time.

Moreover, the activation enthalpy ΔH of stress relaxation at a given stress level can be calculated by the equation: $\Delta H(\sigma) = -\frac{\partial ln(-\dot{\sigma})}{\partial[1/(k_BT)]}$ [36]. As shown in Fig. 2(d), the activation enthalpy of $La_{56.14}Ce_{14.04}Ni_{19.8}Al_{10}$ MG at 32 MPa is 0.46 ± 0.03 eV. The activation enthalpy of stress relaxation is smaller than that of β relaxation (inset of Fig. 1(d)), which may be a consequence of the mechanical work done by stress.

In addition, the correlation between stress and time during stress relaxation process could be described by Ref. [48]:

$$\varphi\sigma(t) = -\frac{k_BT}{V_{act}} ln\left(1 + \frac{t}{C_r}\right), \quad (2)$$

where $\Delta\sigma(t)$ is the stress drop at time t, V_{act} is an apparent activation volume, and C_r is a time constant. The stress drop versus time is shown in Fig. 2(e). According to eq. (2), the values of the apparent activation volume V_{act} and time constant C_r at various temperatures are given in Fig. 2(f). It can be seen that V_{act} takes high values near the temperature range of β relaxation and then keeps stable at around 0.43 nm^3. It means the stress relaxation mechanism becomes less collective at higher temperature. As the temperature increases (around T_g), it shows an upward tendency with temperature once again, which is probably associated with the transition from the secondary β to primary α relaxation. On the other hand, the time constant C_r decreases sharply with increasing temperature, which means that plastic deformation could be activated more easily by increasing temperature. This trend is in agreement with the decreased relaxation time τ_c shown in Fig. 2(b). The apparent activation volume remains at around 0.43 nm^3 over a wide temperature range. Considering that the average atomic volume of the present MG is $\Omega = 0.013$ nm^3 [25], it suggests the activation volume V_{act} for the stress relaxation process in $La_{56.14}Ce_{14.04}Ni_{19.8}Al_{10}$ is about the volume of 33

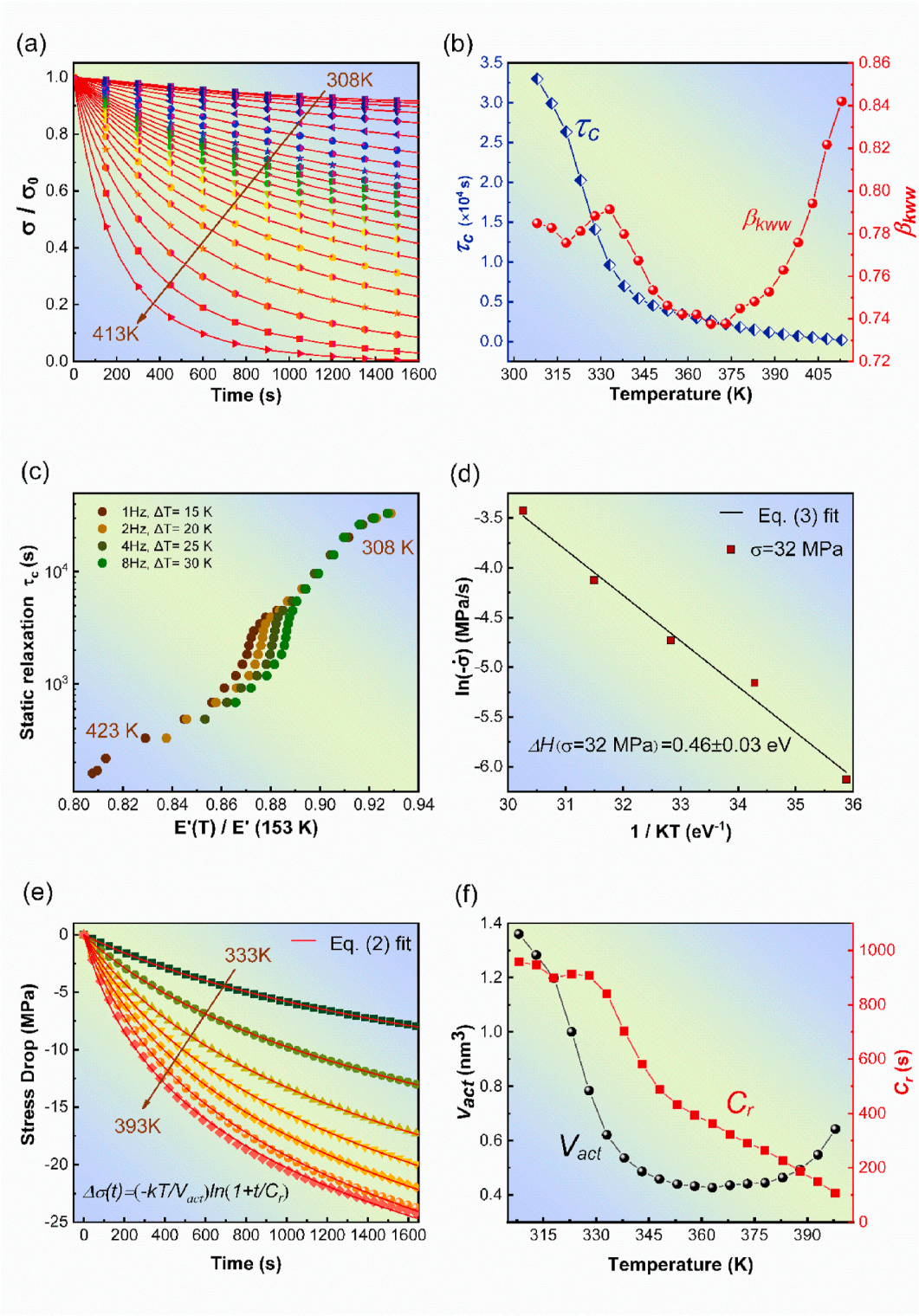

Fig. 2. (a) Stress relaxation of $La_{56.16}Ce_{14.04}Ni_{19.8}Al_{10}$ MGs from 308 to 413 K (temperature interval is 5 K) with at constant strain 0.4%. The stress level was normalized by the initial stress. The solid lines are fitting curves by the KWW function; (b) Variation of fitted KWW parameters τ_c and β_{KWW} with temperature; (c) τ_c as determined from the KWW fit of static relaxation data at different temperatures T as a function of relative bulk modulus determined at temperatures $T+\Delta T$ by DMA; (d) An Arrhenius plot indicates an activation enthalpy of 0.46 ± 0.03 eV at 32 MPa during stress relaxation process; (e) Stress drop relaxation curves of $La_{56.14}Ce_{14.04}Ni_{19.8}Al_{10}$ MG from 333 to 393 K (interval temperature is 10 K) and the solid lines are fitting curves based on eq. (2); (f) Variation of the activation volume V_{act} and the time constant C_r as a function of temperature.

atoms. As suggested by Argon [23], the activation volume is of about 1/10 of the STZ size, then the latter is approximately the size of several hundreds of atoms. It is of great significance to point out that for those MGs without obvious β relaxation such as Zr-, Cu-, and Mg-based ones, the activation volume corresponds to a smaller volume, only around 20 atoms [49]. As such the activation volume might be regarded as an indicator to measure the glass heterogeneity; a higher value may be a consequence of higher "defect" concentration. Accordingly, $La_{56.14}Ce_{14.04}Ni_{19.8}Al_{10}$ MG shows a relatively more inhomogeneous microstructure, which induces a higher defect density, and then triggers a conspicuous β relaxation.

Beside DMA and stress relaxation, creep is another prevalent mechanical technique to probe the structural heterogeneity in MGs [14]. Fig. 3(a) shows the creep behavior under various stresses at a fixed temperature of 330K, while the slopes of the dotted lines in the figure are taken as representatives of the steady-state strain rate. It can be easily seen that as the stress increases, the corresponding steady-state creep strain rate gradually increases. According to the free-volume model [27], the constitutive equation of metallic glasses at high temperature can be described as:

$$\dot{\varepsilon} = 2c_f\nu_D exp\left(-\frac{\Delta G^m}{k_B T}\right)\sinh\left(\frac{\sigma_f V}{2\sqrt{3}k_B T}\right) = \dot{\varepsilon}_0 \sinh\left(\frac{\sigma_f V}{2\sqrt{3}k_B T}\right), \quad (3)$$

where $\dot{\varepsilon}_0 = 2c_f\nu_D exp\left(-\frac{\Delta G^m}{k_B T}\right)$ is a prefactor of strain rate, c_f is the concentration of flow defects, ν_D is the Debye frequency, ΔG^m is the apparent activation energy for defect migration, k_B is the Boltzmann constant, T is the absolute temperature, σ_f is the steady-state flow stress and V denotes the activation volume.

Fig. 3(b) shows the change of steady-state creep strain rate with applied stress at various temperatures, and the solid lines are fitting curves from eq. (3). It should be noted that the activation volume V increases from 0.31 nm^3 at 330 K to about 0.50 nm^3 at 370 K, which means that under the creep stimulation a larger activation volume is activated in the $La_{56.16}Ce_{14.04}Ni_{19.8}Al_{10}$ MG with increasing temperature. At the same temperature of 370 K, the apparent activation volume during the stress relaxation process is 0.44 nm^3. This is a noticeable fact, as both the stress relaxation and the creep processes of

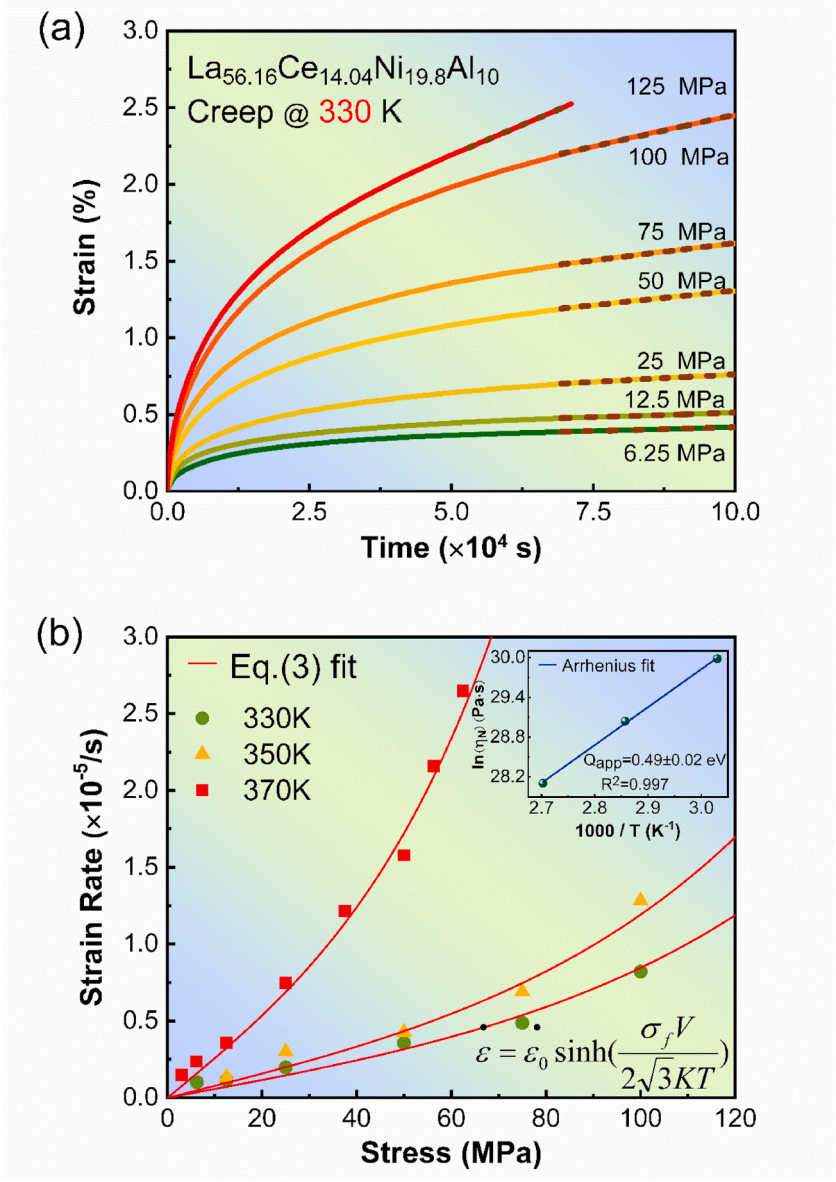

Fig. 3. (a) Creep of $La_{56.16}Ce_{14.04}Ni_{19.8}Al_{10}$ MG at varying stresses at 330 K; (b) Variation of the steady-state creep strain rate with applied stress at different temperatures (330, 350 and 370 K). (Inset: an Arrhenius plot of the calculated Newtonian viscosity *versus* the reciprocal temperature.)

$La_{56.16}Ce_{14.04}Ni_{19.8}Al_{10}$ MG reflect the migration movement of local atomic clusters.

At very high temperature (typically for $T > 0.8T_g$), the viscosity of MGs can be derived as [50]:

$$\eta = \frac{\sigma_f}{3\dot{\varepsilon}} = \frac{\sigma_f}{3\dot{\varepsilon}_0 sinh\left(\frac{\sigma_f V}{2\sqrt{3}k_B T}\right)}. \quad (4)$$

In the Newtonian flow region, the value of $\sigma_f V$ is considerably smaller than thermal energy $k_B T$. Therefore, the term $sinh\left(\frac{\sigma_f V}{2\sqrt{3}k_B T}\right)$ could be approximated by $\frac{\sigma_f V}{2\sqrt{3}k_B T}$. Finally, the Newtonian viscosity η_N can be written as:

$$\eta_N = \frac{2\sqrt{3}k_B T}{3\dot{\varepsilon}_0 V}. \quad (5)$$

According to eq. (3) and eq. (5), Newtonian viscosity η_N can be determined as 1.05×10^{13}, 4.10×10^{12}, 1.61×10^{12} Pa·s for $T =$ 330, 350 and 370 K, respectively. In addition, correlation between the Newtonian viscosity η_N and temperature T follows the Arrhenius equation: $\eta_N = \eta_0 exp\left(\frac{Q_{app}}{k_B T}\right)$, where η_0 is a viscosity constant and Q_{app} is the apparent activation energy of viscous flow. As shown in the inset of Fig. 3(b), the apparent activation energy during creep for $La_{56.16}Ce_{14.04}Ni_{19.8}Al_{10}$ MG obtained from Arrhenius equation is $Q_{app} = 0.49 \pm 0.02$eV. This value is much smaller than that of some MG systems, such as $Zr_{55}Cu_{30}Ni_5Al_{10}$ (5.1 eV) [27] and $Zr_{41.2}Ti_{13.8}Cu_{12.5}Ni_{10}Be_{22.5}$ (4.8 eV) [50]. It is also probably related to the fact that given the inhomogeneous microstructure inside the $La_{56.16}Ce_{14.04}Ni_{19.8}Al_{10}$ MG with pronounced β relaxation, a comparatively lower energy is demanded to start the creep process at temperatures far below T_g. This is probably an evidence that creep in the considered temperature range is driven by β relaxation, the latter originates from the structural inhomogeneity in glass.

To deepen into the creep mechanisms, the relaxation spectrum of the creep process, which directly reflects the dynamic heterogeneity, was computed. The creep strain curves were fitted to a sum of Kelvin-Voigt units of increasing relaxation times:

$$\varepsilon(t) = \sum_{i=1}^{N} \varepsilon_0 [1 - exp(-t/\tau_i)], \quad (6)$$

with $1\ s < \tau_i < 10^{10}$ s and $N = 40$. The fitting procedure was chosen to enhance the maximum likelihood of the determined relaxation times. Fig. 4 shows the intensities of the fitted relaxation times as a function of both applied stress and temperature in the studied range. It can be seen that the relaxation modes remain the same in the studied range, showing no dependence in temperature. This result, combined with the observed increase of the activation volume for creep as temperature increases supports the picture that the flow units being activated by creep are similar in the examined temperature range. Therefore, no coalescence between flow units is found in the studied temperature range, which is compatible with the hypothesis that creep is mediated by β relaxation. This is also coherent with the reported fact that glasses having noticeable β relaxation show better plasticity. In fact, the apparent creep activation energy of $La_{56.16}Ce_{14.04}Ni_{19.8}Al_{10}$ is lower than the activation energy of the β relaxation as found in other MGs [24], which reinforces the hypothesis that glasses showing large β relaxation show also better plasticity.

4. Conclusions

In summary, DMA, stress relaxation and creep experiments were launched within a wide range of temperature to investigate the deformation mechanism and the evolution of microstructural heterogeneity of the $La_{56.16}Ce_{14.04}Ni_{19.8}Al_{10}$ MG under various forms of mechanical stimuli. Several theoretical approaches have been used to investigate the evolution of the microstructural heterogeneity with temperature of LaCe-based MG. These theoretical approaches allow us to go further than the pure macroscopic description and obtain numerous physical quantities which can give an insight on the micro-structure information. However, these theoretical methods are sometimes phenomenological without explicit physical input. Besides, one is required to pay more attention to the temperature range or other restrictions when using them, owing to the fact that these models are constructed by assuming homogeneous deformation of the material. An apparent β relaxation activation energy E_β of 0.762 eV has been calculated. A relatively high value of the stress relaxation activation volume of about 0.43 nm^3 has been stimulated, implying a high defect concentration and a largely

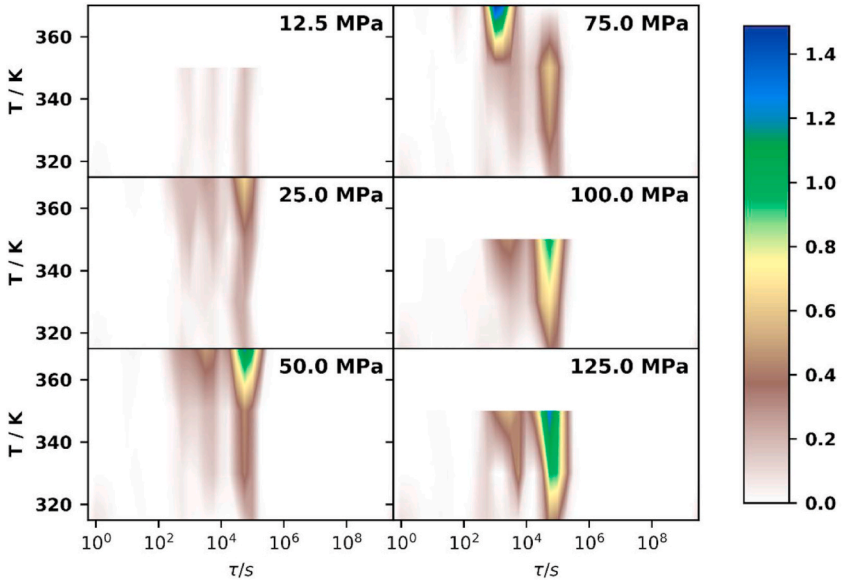

Fig. 4. Heat map plot of the intensity of the relaxation times in creep of $La_{56.16}Ce_{14.04}Ni_{19.8}Al_{10}$ MG at different applied stresses as a function of temperature. The color bar denotes the magnitude of relative intensity.

inhomogeneous microstructure. The fitted parameter β_{KWW} shows an increasing tendency as the temperature approaches the glass transition, which corresponds to the emergence of a more homogeneous microstructure at higher temperature. Moreover, a correlation was found between the bulk modulus of the glass and the main relaxation time τ_c, revealing the common plasticity mechanism. The activation enthalpy of stress relaxation is 0.46 eV, while the activation energy during creep process is 0.55 eV, and the creep mechanism at low temperatures appears to be controlled by β relaxation. Our results reveal that $La_{56.16}Ce_{14.04}Ni_{19.8}Al_{10}$ MG shows a similar deformation mechanism under various forms of external stimuli, which links the slow β relaxation, plastic deformation, as well as structural heterogeneity in MGs.

Declaration of competing interest

The authors declare that they have no known competing financial interests or personal relationships that could have appeared to influence the work reported in this paper.

Acknowledgements

This work is supported by the NSFC (Grant Nos. 51971178 and 11672299), the research of JCQ was supported by the Fundamental Research Funds for the Central Universities (Nos. 3102019ghxm007 and 3102017JC01003), Astronautics Supporting Technology Foundation of China (2019-HT-XG), the Natural Science Foundation of Shaanxi Province (No. 2019JM-344) and Opening fund of State Key Laboratory of Nonlinear Mechanics (LNM201911). D.C. and E.P. acknowledge the financial support from MINECO (grant FIS2017-82625-P) and Generalitat de Catalunya (grant 2017SGR0042). YJW was supported by the Youth Innovation Promotion Association of Chinese Academy of Sciences (Grant No. 2017025).

References

[1] W.H. Wang, The elastic properties, elastic models and elastic perspectives of metallic glasses, Prog. Mater. Sci. 57 (3) (2012) 487–656.
[2] A. Inoue, A. Takeuchi, Recent development and application products of bulk glassy alloys, Acta Mater. 59 (6) (2011) 2243–2267.
[3] Y. Wu, H. Bei, Y.L. Wang, Z.P. Lu, E.P. George, Y.F. Gao, Deformation-induced spatiotemporal fluctuation, evolution and localization of strain fields in a bulk metallic glass, Int. J. Plast. 71 (2015) 136–145.
[4] C. Chang, J. Zhang, B. Shen, W. Wang, A. Inoue, Pronounced enhancement of glass-forming ability of Fe–Si–B–P bulk metallic glass in oxygen atmosphere, J. Mater. Res. 29 (10) (2014) 1217–1222.
[5] J.C. Qiao, Q. Wang, D. Crespo, Y. Yang, J.M. Pelletier, Secondary relaxation and dynamic heterogeneity in metallic glasses: a brief review, Chin. Phys. B 26 (1) (2017), 016402.
[6] M.W. Chen, Mechanical behavior of metallic glasses: microscopic understanding of strength and ductility, Annu. Rev. Mater. Res. 38 (2008) 445–469.
[7] S.H. Hong, J.T. Kim, S.C. Mun, Y.S. Kim, H.J. Park, Y.S. Na, K.R. Lim, J.M. Park, K. B. Kim, Influence of spherical particles and interfacial stress distribution on viscous flow behavior of Ti-Cu-Ni-Zr-Sn bulk metallic glass composites, Intermetallics 91 (2017) 90–94.
[8] S.H. Hong, J.T. Kim, H.J. Park, Y.S. Kim, J.Y. Suh, Y.S. Na, K.R. Lim, J.M. Park, K. B. Kim, Gradual martensitic transformation of B2 phase on TiCu-based bulk metallic glass composite during deformation, Intermetallics 75 (2016) 1–7.
[9] G. Song, C. Lee, S.H. Hong, K.B. Kim, S. Chen, D. Ma, K. An, P.K. Liaw, Martensitic transformation in a B2-containing CuZr-based BMG composite revealed by in situ neutron diffraction, J. Alloys. Compd. 723 (2017) 714–721.
[10] K.S. Lee, S. Kim, K.R. Lim, S.H. Hong, K.B. Kim, Y.S. Na, Crystallization, high temperature deformation behavior and solid-to-solid formability of a Ti-based bulk metallic glass within supercooled liquid region, J. Alloys Compd. 663 (2016) 270–278.
[11] A.L. Greer, Y.Q. Cheng, E. Ma, Shear bands in metallic glasses, Mater. Sci. Eng. R 74 (4) (2013) 71–132.
[12] D. Wei, J. Yang, M.Q. Jiang, Revisiting the structure–property relationship of metallic glasses: common spatial correlation revealed as a hidden rule, Phys. Rev. B 99 (2019), 014115.
[13] V. Bapst, T. Keck, Grabska-Barwińska, Unveiling the predictive power of static structure in glassy systems, Nat. Phys. 16 (2020) 448–454.
[14] J.C. Qiao, Q. Wang, J.M. Pelletier, H. Kato, R. Casalini, D. Crespo, E. Pineda, Y. Yao, Y. Yang, Structural heterogeneities and mechanical behavior of amorphous alloys, Prog. Mater. Sci. 104 (2019) 250–329.
[15] H. Wagner, D. Bedorf, S. Kuchemann, M. Schwabe, B. Zhang, W. Arnold, K. Samwer, Local elastic properties of a metallic glass, Nat. Mater. 10 (6) (2011) 439–442.
[16] Y.H. Liu, D. Wang, K. Nakajima, W. Zhang, A. Hirata, T. Nishi, A. Inoue, M. W. Chen, Characterization of nanoscale mechanical heterogeneity in a metallic glass by dynamic force microscopy, Phys. Rev. Lett. 106 (12) (2011) 125504.
[17] P. Tsai, K. Kranjc, K.M. Flores, Hierarchical heterogeneity and an elastic microstructure observed in a metallic glass alloy, Acta Mater. 139 (2017) 11–20.
[18] H.B. Yu, W.H. Wang, K. Samwer, The β relaxation in metallic glasses: an overview, Mater. Today 16 (2013) 183–191.
[19] Y.H. Liu, G. Wang, R.J. Wang, D.Q. Zhao, M.X. Pan, W.H. Wang, Super plastic bulk metallic glasses at room temperature, Science 315 (5817) (2007) 1385–1388.
[20] F. Zhu, H.K. Nguyen, S.X. Song, D.P. Aji, A. Hirata, H. Wang, K. Nakajima, M. W. Chen, Intrinsic correlation between beta-relaxation and spatial heterogeneity in a metallic glass, Nat. Commun. 7 (2016) 11516.
[21] H.B. Yu, W.H. Wang, H.Y. Bai, Y. Wu, M.W. Chen, Relating activation of shear transformation zones to β relaxations in metallic glasses, Phys. Rev. B 81 (22) (2010) 220201, 4.
[22] H.T. Hiroshi Shintani, Frustration on the way to crystallization in glass, Nat. Phys. 2 (2006) 200–206.
[23] A.S. Argon, Plastic deformation in metallic glasses, Acta Metall. 27 (1979) 47–58.
[24] H.B. Yu, X. Shen, Z. Wang, L. Gu, W.H. Wang, H.Y. Bai, Tensile plasticity in metallic glasses with pronounced β relaxations, Phys. Rev. Lett. 108 (1) (2012), 015504.
[25] J.C. Qiao, Y.J. Wang, J.M. Pelletier, L.M. Keer, M.E. Fine, Y. Yao, Characteristics of stress relaxation kinetics of $La_{60}Ni_{15}Al_{25}$ bulk metallic glass, Acta Mater. 98 (2015) 43–50.
[26] T.S. Yoshihito Kawamura, Akihisa Inoue, Tsuyoshi Masumoto, Stress overshoot in stress-strain curves of $Zr_{65}Al_{10}Ni_{10}Cu_{15}$ metallic glass, Mater. Trans. JIM 40 (1999) 335–342.
[27] F. Spaepen, Microscopic mechanism for steady state inhomogeneous flow in metallic glasses, Acta Metall. 25 (1977) 407–415.
[28] H. Zou, H. Trevor, Regularization and variable selection via the elastic net, J. Roy. Stat. Soc. B 67 (2005) 301–320.
[29] W.H. Wang, Dynamic relaxations and relaxation-property relationships in metallic glasses, Prog. Mater. Sci. 106 (2019) 100561.
[30] Q. Wang, S.T. Zhang, Y. Yang, Y.D. Dong, C.T. Liu, J. Lu, Unusual fast secondary relaxation in metallic glass, Nat. Commun. 6 (1) (2015).
[31] M.D. Demetriou, J.S. Harmon, M. Tao, G. Duan, K. Samwer, W.L. Johnson, Cooperative shear model for the rheology of glass-forming metallic liquids, Phys. Rev. Lett. 97 (6) (2006), 065502.
[32] J.C. Qiao, B.A. Sun, J. Gu, M. Song, J.M. Pelletier, J.W. Qiao, Y. Yao, Y. Yang, Abnormal internal friction in the in-situ Ti60Zr15V10Cu5Be10 metallic glass matrix composite, J. Alloys Compd. 724 (2017) 921–931.
[33] G.J. Lyu, J.C. Qiao, J.M. Pelletier, Y. Yao, The dynamic mechanical characteristics of Zr-based bulk metallic glasses and composites, Mater. Sci. Eng. A 711 (2018) 356–363.
[34] L. Chen, C.R. Cao, J.A. Shi, Z. Lu, Y.T. Sun, P. Luo, L. Gu, H.Y. Bai, M.X. Pan, W. H. Wang, Fast surface dynamics of metallic glass enable superlattice like nanostructure growth, Phys. Rev. Lett. 118 (1) (2017), 016101.
[35] Z. Wang, B.A. Sun, H.Y. Bai, W.H. Wang, Evolution of hidden localized flow during glass-to-liquid transition in metallic glass, Nat. Commun. 5 (2014) 5823.
[36] J.C. Qiao, Y.J. Wang, L.Z. Zhao, L.H. Dai, D. Crespo, J.M. Pelletier, L.M. Keer, Y. Yao, Transition from stress-driven to thermally activated stress relaxation in metallic glasses, Phys. Rev. B 94 (10) (2016) 104203, 9.
[37] J.C. Qiao, J.M. Pelletier, Y. Yao, Creep in bulk metallic glasses. Transition from linear to non linear regime, Mater. Sci. Eng. A 743 (2019) 185–189.
[38] W. Jiao, P. Wen, H.L. Peng, H.Y. Bai, B.A. Sun, W.H. Wang, Evolution of structural and dynamic heterogeneities and activation energy distribution of deformation units in metallic glass, Appl. Phys. Lett. 102 (10) (2013) 101903.
[39] S.T. Liu, W. Jiao, B.A. Sun, W.H. Wang, A quasi-phase perspective on flow units of glass transition and plastic flow in metallic glasses, J. Non-Cryst. Solids 376 (2013) 76–80.
[40] Z. Lu, W. Jiao, W.H. Wang, H.Y. Bai, Flow unit perspective on room temperature homogeneous plastic deformation in metallic glasses, Phys. Rev. Lett. 113 (4) (2014), 045501.
[41] T. Egami, Atomic level stresses, Prog. Mater. Sci. 56 (6) (2011) 637–653.
[42] T. Egami, Mechanical failure and glass transition in metallic glasses, J. Alloys. Compd. 509 (2011) S82–S86.
[43] J. Perez, Quasi-punctual defects in vitreous solids and liquid-glass transition, Solid State Ionics 39 (1990) 69–79.
[44] J. Perez, S. Etienne, J. Tatibouet, Determination of glass transition temperature by internal friction measurements, Phys. Status Solidi 121 (1990) 129–138 (a).
[45] C. Zhang, J.C. Qiao, J.M. Pelletier, Y. Yao, Thermal activation in the $Zr_{65}Cu_{18}Ni_7Al_{10}$ metallic glass by creep deformation and stress relaxation, Scripta Mater. 113 (2016) 180–184.
[46] Y. Tong, J.C. Qiao, C. Zhang, J.M. Pelletier, Y. Yao, Mechanical properties of $Ti1_{6.7}Zr_{16.7}Hf_{16.7}Cu_{16.7}Ni_{16.7}Be_{16.7}$ high-entropy bulk metallic glass, J. Non-Cryst. Solids 452 (2016) 57–61.
[47] J.C. Qiao, Y. Yao, J.M. Pelletier, L.M. Keer, Understanding of micro-alloying on plasticity in Cu 46 Zr 47−x Al 7 Dy x (0≤ x ≤ 8) bulk metallic glasses under compression: based on mechanical relaxations and theoretical analysis, Int. J. Plast. 82 (2016) 62–75.

[48] D. Caillard, J.L. Martin, Thermally Activated Mechanisms in Crystal Plasticity, Elsevier, 2003, pp. 15–20.
[49] J.C. Qiao, J.M. Pelletier, J.J. Blandin, S. Gravier, High temperature deformation in a lanthanum based bulk metallic glass showing a pronounced secondary relaxation, Mater. Sci. Eng. A 586 (2013) 57–61.
[50] M. Bletry, P. Guyot, J.J. Blandin, J.L. Soubeyroux, Free volume model: high-temperature deformation of a Zr-based bulk metallic glass, Acta Mater. 54 (5) (2006) 1257–1263.